Carbohydrate Polymers 102 (2014) 136–143

Contents lists available at ScienceDirect

Carbohydrate Polymers

journal homepage: www.elsevier.com/locate/carbpol

Preparation and characterization of cellulose nanofibers from de-pectinated sugar beet pulp

Meng Li[a,1], Li-jun Wang[b,1], Dong Li[a,*], Yan-Ling Cheng[c,*], Benu Adhikari[d]

[a] College of Engineering, National Energy R&D Center for Non-food Biomass, China Agricultural University, P.O. Box 50, 17 Qinghua Donglu, Beijing 100083, China
[b] College of Food Science and Nutritional Engineering, Beijing Key Laboratory of Functional Food from Plant Resources, China Agricultural University, Beijing, China
[c] College of Biochemical Engineering, Beijing Union University, Beijing 100023, China
[d] School of Applied Sciences, RMIT University, City Campus, Melbourne, VIC 3001, Australia

ARTICLE INFO

Article history:
Received 30 September 2013
Received in revised form 5 November 2013
Accepted 16 November 2013
Available online 25 November 2013

Keywords:
Cellulose nanofibers
Sugar beet
High pressure homogenization
Morphology
Thermal degradation

ABSTRACT

Cellulose nanofibers (diameter = 10–70 nm) were produced using chemical treatments (alkali treatment and bleaching) and high pressure homogenization from de-pectinated sugar beet pulp (DSBP). Chemical analysis and Fourier transform infrared spectroscopy (FTIR) indicated that the chemical treatments greatly removed the hemicellulose and lignin from the DSBP and significantly increased the cellulose content. The crystallinity of the cellulose nanofibers increased from 35.67% to 69.62% after alkali treatment and bleaching. The thermal degradation temperature of DSBP cellulose nanofibers was 271.7 °C which was found to be 47.3 °C higher than that of the untreated DSBP. The DSBP cellulose nanofibers can be preferably used as reinforcement in the biocomposite material at high temperature.

1. Introduction

With growing environmental awareness and energy demands, there is an increasing interest to produce low-cost, biodegradable and environment friendly materials derived from renewable agricultural waste or agro-industrial byproducts. Cellulose is one of the most abundant polysaccharides in nature and it is non-toxic, biodegradable and comes from renewable source. Chemically, cellulose is composed of D-glucose units linked with unbranched β-(1-4)-glycosidic bond (Kim, Yun, & Ounaies, 2006). It is organized into microfibril in the cell wall, interrupted by hemicellulose and surrounded by a lignin matrix. A number of common plants such as cotton, wood, bamboo, henequen, flax, hemp, sisal, and jute are rich in cellulose. In recent years, these natural cellulose fibers are increasingly being used as reinforcing materials in thermoset and thermoplastic polymeric matrices (Abe, Iwamoto, & Yano, 2007; Siqueira, Bras, & Dufresne, 2008; Soykeabkaew, Supaphol, & Rujiravanit, 2004). Therefore, composite products reinforced by natural fibers can be used to replace composite products reinforced by synthetic fibers in automotive, packaging, and furniture making industries. Cellulose nanofibers have drawn increased attention because of their unique characteristics, such as large surface to volume ratio and excellent thermomechanical properties including high tensile strength, high Young's modulus and low coefficient of thermal expansion (Azizi Samir, Alloin, & Dufresne, 2005; Nishino, Matsuda, & Hirao, 2004). All of these features make cellulose nanofibers a promising material in the field of nanotechnology.

Nanometer-sized cellulose fibers or crystals can be obtained from various natural materials which are rich in cellulose such as rice straw and potato (Abe & Yano, 2009), raw kenaf fibers (Jonoobi, Harun, Mathew, Hussein, & Oksman, 2010), wheat straw and soy hulls (Alemdar & Sain, 2008), coconut husk (Rosa et al., 2010) and aquatic weeds (Thiripura Sundari & Ramesh, 2012). The cellulose nanofibers produced from these agro-industrial byproducts are widely used in diverse industrial applications such as food (Okiyama, Motoki, & Yamanaka, 1993), pharmaceutical (Villanova et al., 2011), packaging (Bradley, Castle, & Chaudhry, 2011), film (Syverud, Chinga-Carrasco, Toledo, & Toledo, 2011), paper (Nogi, Iwamoto, Nakagaito, & Yano, 2009) and nanocomposite (Azizi Samir et al., 2005; Faruk, Bledzki, Fink, & Sain, 2012; Iwamoto, Abe, & Yano, 2008) industries.

A number of methods have been applied to obtain cellulose micro/nanofibers from cellulosic materials. Enzymatic hydrolysis (Pääkkö et al., 2007) and acid hydrolysis (sulfuric or hydrochloric

* Corresponding authors. Tel.: +86 10 62737351; fax: +86 10 62737351.
E-mail addresses: dongli@cau.edu.cn (D. Li), cheng1012cn@yahoo.com.cn (Y.-L. Cheng).
[1] These authors contributed equally to this work.

0144-8617/$ – see front matter © 2013 Elsevier Ltd. All rights reserved.
http://dx.doi.org/10.1016/j.carbpol.2013.11.021

acid) (Corrêa, de Morais Teixeira, Pessan, & Mattoso, 2010) have been the most commonly used chemical methods. High shear homogenization (Kaushik & Singh, 2011), grinding (Nogi et al., 2009), high pressure homogenization (Nakagaito & Yano, 2008), microfluidization (Siqueira et al., 2008) and sonication (Chen et al., 2011) have been the most commonly used mechanical methods. Application of these methods was found to result into nanofibrillar material having different characteristics depending on the raw material, treatment method and the disintegration process (Chen et al., 2011; Corrêa et al., 2010).

High pressure homogenization (HPH) is an economic and efficient production technology applied to produce cellulose nanofibers. During HPH process, the aqueous suspension of pulp fibers experiences high pressure, high shear, turbulence, and cavitation caused by rapid change in pressure when the samples pass through the homogenization chamber (Wang, Li, Wang, Liu, & Adhikari, 2012). The integral effect of high pressure, high shear, turbulence and cavitation during the HPH process disintegrates amorphous regions, reduces the size of cellulose fibers, further disperses the disintegrated fraction, causes total disruption of cells and ultimately releases cellulose nanofibers.

There are no publications suggesting that sugar beet pulp (SBP) can be used as a source to extract cellulose nanofibers. SBP is a byproduct of beet sugar industry and is produced in large quantity every year. About 10 million tons/year of SBP is left after extracting sugar from sugar beet in China (Jin, 2004). Pectin can be successfully extracted from SBP (Lv, Wang, Wang, Li, & Adhikari, 2013). De-pectinated SBP (DSBP) is a very important biomaterial consisting 40–50% cellulose, 20–30% hemicellulose and a small percentage of lignin. Therefore, in order to better utilize the SBP, the potential of DSBP for the production of nanofibers deserves a systematic investigation.

In this paper, we aimed at isolating cellulose fibers from DSBP using alkali and bleaching treatments. Then, the cellulose nanofibers were produced from the DSBP cellulose fibers using high pressure homogenization. The composition of the cellulose nanofibers was determined by chemical analysis and FTIR. The morphological features and crystal structure of the cellulose nanofibers were investigated using scanning electron microscopic (SEM), transmission electron microscopic (TEM) and X-ray diffraction (XRD) techniques. The thermogravimetric analysis was used to determine the thermal stability of the isolated DSBP cellulose nanofibers.

2. Materials and methods

2.1. Materials

Sugar beet pulp (SBP) was obtained from Xinjiang Province of China. Benzene, absolute ethanol, sodium hydroxide (NaOH), sodium chlorite ($NaClO_2$) and other chemicals were of analytical grade and were supplied by Beijing Chemical Works (Beijing, China).

2.2. Isolation of cellulose fibers (CFs) from DSBP

2.2.1. Alkali treatment

The DSBP powder was produced by following a method suggested by Lv et al. (2013). This powder was sieved under 80 mesh sieve and dried to the constant weight. DSBP powder was first extracted with a 2:1 (v/v) mixture of toluene and ethanol for 6 h to remove wax and oil. The dewaxed sample was then treated with 4% (w/v) NaOH for 2 h. The residual was then filtered and washed with distilled water several times until its pH was neutral.

2.2.2. Bleaching treatment

After alkali treatment, the bleaching process was used to remove the lignin. Five (5) g of the alkali treated sample was heated for 1 h at 70–80 °C together with 160 ml of water containing 1.5 g of sodium chlorite and 10 drops of glacial acetic acid. This step was repeated for three times. Finally, the pulp was filtered and washed with distilled water until it had a neutral pH.

2.2.3. Preparation of cellulose nanofibers

The bleached pulp fibers were homogenized using a high-pressure homogenizer (AH 100D, ATS Engineering Inc., Italy). The sample was diluted to 0.5% (w/v) with distilled water, and then passed through the high-pressure homogenizer at 200 bar (20.37 MPa absolute pressure). This step was carried out to avoid clogging during homogenization. The sample was then passed through the homogenizer 10 times at 800 bar (81.16 MPa, absolute pressure). Finally, the homogenized samples were lyophilized to obtain the cellulose nanofibers.

2.3. Characterization of sugar beet fibers and nanofibers

2.3.1. Chemical composition

The chemical composition of DSBP at each stage of treatment was determined according to the standards provided by Technical Association of Pulp and Paper Industry (TAPPI). The percentage of holocellulose (cellulose + hemicellulose) was determined by the method proposed by Wise et al. (1946). The α-cellulose and lignin (acid-insoluble) contents were measured according to TAPPI T203 and TAPPI T222 methods, respectively. The hemicellulose content was calculated from the difference between holocellulose and α-cellulose values. Triplicate tests were carried out and the averaged values are reported in ensuing sections.

2.3.2. Characterization of morphological features

The morphology and microstructure of the cellulose microfibers and nanofibers were characterized using scanning electron microscope (JSM-5800, JEOL Co., Ltd., Japan). Samples were fixed on a metal stub with double-sided tape and the surface of these samples was coated with platinum. Images were taken at 15 kV accelerating voltage.

The dimension of the cellulose nanofibers was determined by using transmission electron microscope (TEM) (H-7650B, Hitachi High-Technologies, Japan). A drop of diluted cellulose nanofibers suspension was placed on the surface of a carbon-coated copper grid. Then, the cellulose nanofibers were negatively stained with uranyl acetate for 1 min and allowed to dry at ambient temperature. TEM images were taken at an accelerating voltage of 80 kV.

The diameter of the cellulose fibers after homogenization treatment was calculated by a digital image processing program (Image J, National Institute of Health, USA).

2.3.3. Fourier transform infrared spectroscopy (FTIR)

FTIR analysis of DSBP at each stage of treatment was carried out to examine any alterations in the structure of the fibers before and after treatments. FTIR spectra were measured using a FTIR spectrometer (Spectrum 100™, PerkinElmer, USA) at ambient conditions. The samples were crushed into powder and mixed with potassium bromide (KBr) (1:100, w/w) to prepare pastilles for FTIR analysis. FTIR spectra were recorded in transmittance mode at a resolution of 4 cm^{-1} from 4000 cm^{-1} to 400 cm^{-1}. Total 32 scans were taken for each sample. Three repeat runs were carried out to compare the FTIR signals.

2.3.4. X-ray diffraction (XRD) analysis

The crystallinity of the samples was determined by using an X-ray diffractometer (XD-2, Beijing Purkinje General Instrument Co.,

Ltd., China) using Ni-filtered Cu Kα radiation (λ = 0.15406 nm) at an operating voltage of 36 kV and a filament current of 20 mA. XRD samples were prepared by pressing sample into the sample holder with 2 mm hole in the middle. The samples were scanned in 2θ angles from 5° (2θ) to 40° (2θ) with a scanning rate of 1°/min, and step size is 0.02° at ambient condition. The crystallinity index (CI) was calculated using the Segal method given by Eq. (1) below (Segal, Creely, Martin, & Conrad, 1959):

$$\text{CI}\ \ (\%) = 100 \times \frac{I_{0\,02} - I_{\text{am}}}{I_{002}} \quad (1)$$

where I_{002} is the maximum intensity of the principal peak (2 0 0) lattice diffraction (2θ = 22°), and I_{am} is the diffraction intensity of amorphous cellulose between the plane (2 0 0) and (1 1 0) (2θ = 18°). The diffraction peak for plane (0 0 2) is around 2θ = 22° representing both crystalline and amorphous regions and the intensity of the amorphous region is measured around 2θ = 18°.

2.3.5. Thermogravimetric analysis

Thermogravimetric analysis (TGA) was performed to quantify the degradation characteristics (or thermal stability) of cellulose fibers obtained from different treatments. The thermal stability experiments were performed using a thermogravimetric analyzer (Q5000 series, TA Instruments, USA) under a nitrogen atmosphere with a gas flow rate of 35 ml/min. Each sample was heated from ambient temperature to 700 °C at a heating rate of 10 °C/min.

2.3.6. Statistical analysis

All the experiments were carried out in triplicate. The data of chemical composition were expressed as mean ± standard deviation. The results were analyzed by analysis of variance (ANOVA). Duncan's multiple comparison tests were used to determine the significance difference between the mean values. A confidence level of 95% ($p < 0.05$) was used and the analyses were carried out using SPSS 17.0 software (SPSS Inc., Chicago, USA).

3. Results and discussion

3.1. Chemical analysis

The chemical composition of the DSBP samples at each stage of purification treatment is listed in Table 1. It can be seen from this table that the chemical treatments have a significant effect ($p < 0.05$) on the chemical composition of these samples. The untreated DSBP had a lower percentage of α-cellulose (44.96%) and higher percentages of hemicellulose (25.40%) and lignin (11.23%) compared to that of the chemically treated samples. After the alkali treatment, the α-cellulose content increased to 70.85%, while the hemicellulose and lignin contents decreased to 9.32% and 8.67%, respectively. This extent of enrichment of α-cellulose content is due to the fact that alkali treatment partially removes hemicellulose and lignin contents from the surface of the cell wall. The mercerized fibers were then subjected to bleaching treatment. After this bleaching step, lignin content was completely removed, and hemicellulose content was significantly reduced (7.01%), which resulted into significantly enriched (82.83%) cellulose fibers. The above observations indicate that the chemical treatments (alkali treatment followed by bleaching) can breakdown the lignocellulosic structure, promote the hydrolysis of hemicellulose, lead to the cleavage of hemicellulose-lignin bonds and result into complete removal of lignin. This significant ($p < 0.05$) increase in cellulose content brings about greatly improved crystallinity of samples as well as greatly improved thermal properties (Alemdar & Sain, 2008). This aspect will be further discussed in Sections 3.4 and 3.5.

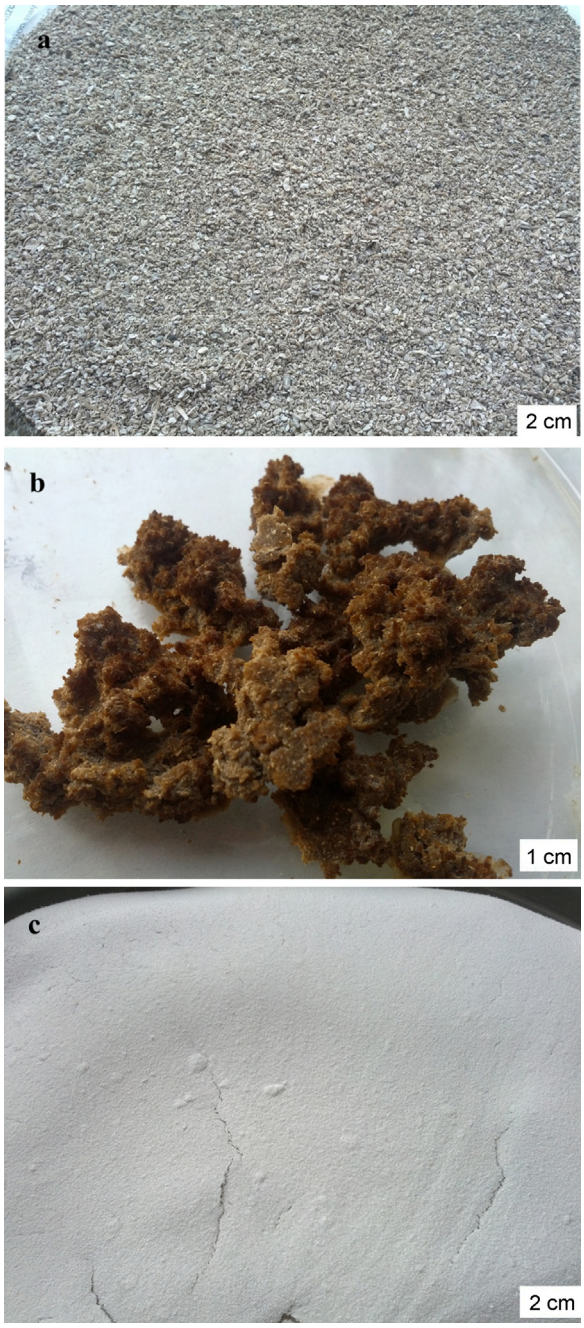

Fig. 1. Photographs of DSBP: (a) untreated DSBP, (b) alkali treated DSBP, and (c) bleached DSBP.

3.2. Morphological characteristics

Fig. 1 shows the macroscopic images of DSBP at different processing stages. The gray color of the untreated DSBP changed into brown after the alkali treatment. The color of the DSBP became completely white after bleaching. The variation of the color of DSBP along the treatment stages reflects the changes in chemical composition in which the non-cellulosic materials such as hemicellulose, lignin, wax and oils were removed due to alkali treatment and bleaching. The final product (after bleaching) appears to be white which indicates that the cellulose content is greatly enriched in the bleached sample, agreeing with its chemical composition (Table 1).

The chemical treatments applied to enrich the cellulose bring about structural changes on the surface of DSBP fibers together with chemical changes. It is also expected that the high pressure

Table 1
Chemical composition of DSBP samples at each stage of treatment.

Materials	Cellulose (%)	Hemicellulose (%)	Lignin (%)	Ash (%)
Untreated fibers	44.95 ± 0.09[a]	25.40 ± 2.06[a]	11.23 ± 1.66[a]	17.67 ± 1.54[a]
Alkali treated fibers	70.85 ± 0.35[b]	9.32 ± 0.65[b]	8.67 ± 0.50[b]	12.78 ± 1.06[b]
Bleached fibers	82.83 ± 3.81[c]	7.01 ± 1.64[c]	0[c]	10.73 ± 0.95 [c]

Values of the chemical composition represent the mean ± standard deviation of three replicates.
Values in a column having different superscripts were significantly different ($p < 0.05$).

homogenization (HPH) also impacts the morphological features of resultant DSBP cellulose fibers. Fig. 2 presents the SEM micrographs of DSBP fibers taken before and after each treatment. It can be observed from these micrographs that the morphological features of untreated and treated DSBP samples are quite different. The surface of the untreated DSBP is smooth and the diameter of the fibers varies between 10 and 25 μm. This observation indicates that the cellulose fibers in the untreated DSBP are held together by pectin, hemicellulose and lignin which are known to act as "natural binders" of cellulose fibers (Kaliyan & Vance Morey, 2009). As can be seen from Fig. 2b, the SBP sample was converted into a network of slender fibrils, and the surface of DSBP (after alkali treatment) becomes rougher, indicating that the partial dissolution of non-cellulosic components such as pectin, hemicellulose, lignin, wax, and other impurities and swelling of cellulose take place during alkali treatment. However, a small number of cellulose fibers are still attached together and the alkali treatment does not appear to completely separate the cellulose fibers free by adequately breaking the cellular structure. This is because the residual lignin acts as a binder by forming a bridging bond with cellulose ester in lignocellulosic plants (Johar, Ahmad, & Dufresne, 2012). Upon bleaching treatment (Fig. 2c), the SBP fiber bundles are partially broken and separated into individual fibers. This is because of the further elimination of cementing materials (hemicellulose + lignin) under strong bleaching conditions. These morphological features indicate that the alkali treatment alone is not capable of removing the non-cellulosic materials to a desired extent. When Fig. 2c and d are compared, it can be observed that the application of HPH affects the structure of DSBP. The network structure of fibers was destroyed and the cellulose fibers were effectively crushed into individual fibers and the diameter of the fibers was decreased to nanometer scale after the HPH treatment. However, a number of cellulose nanofibers aggregated together due to evaporation of water during the drying process, which resulted into a number of large bundles.

The TEM micrograph of cellulose nanofibers subjected to alkali treatment, bleaching and HPH treatment is shown in Fig. 3. The TEM micrograph clearly shows that the HPH treatment resulted into defibrillation of the cellulose nanofibers from the cell wall and helped to release the nanofibers. The TEM image of the cellulose nanofibers shows the opening up of the fiber-bundle and the separation of cellulose fibers down to the nanometer scale. The diameter of cellulose fibers ranged from <10 nm to70 nm, and the diameter of most of fibers was within 10–20 nm. Fig. 3b presents size (diameter) distribution of cellulose nanofibers. Almost 64% of fibers have a diameter within 10–20 nm range. Only 3% of fibers had diameter higher than 50 nm and 14% of fibers had diameter lower than 10 nm.

3.3. The FTIR analysis

Fig. 4 shows the FTIR spectra of untreated DSBP, alkali treated DSBP, bleached DSBP, and cellulose nanofibers. The absorbance peak near 3340–3367 cm^{-1}, observed in all spectra, represents the stretching vibration of O—H (Sain & Panthapulakkal, 2006). A broad absorption band between 3600 cm^{-1} and 3000 cm^{-1} is due to the vibration of hydrogen-bonded hydroxyl groups in the structure

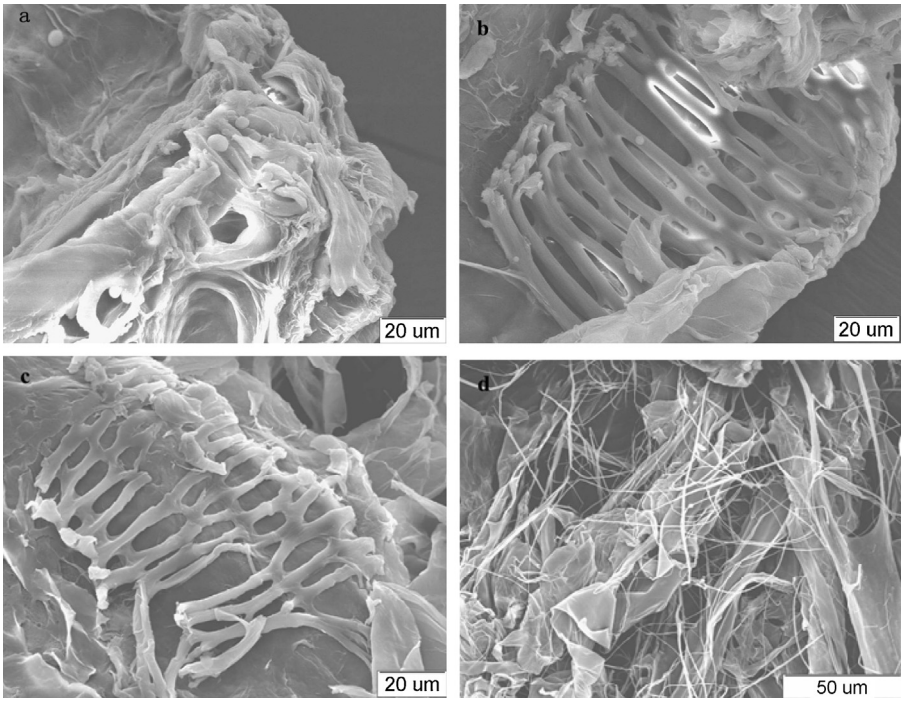

Fig. 2. Scanning electron micrographs of (a) untreated DSBP fibers, (b) alkali treated DSBP fibers, (c) bleached DSBP fibers, and (d) HPH treated DSBP.

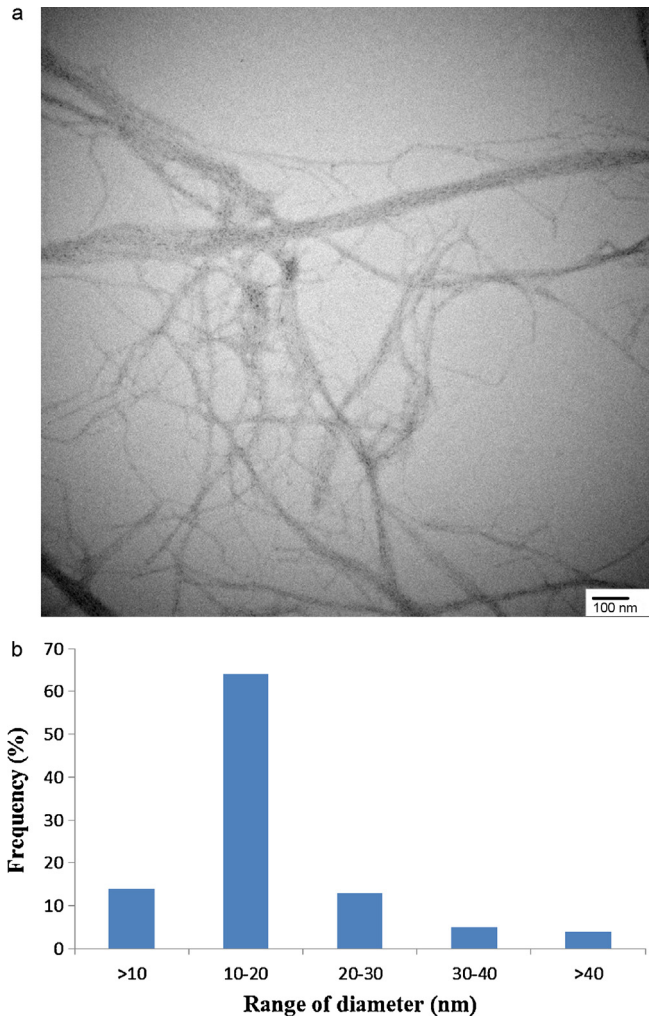

Fig. 3. (a) Transmission electron microscope image and (b) size (diameter) distribution of the cellulose nanofibers.

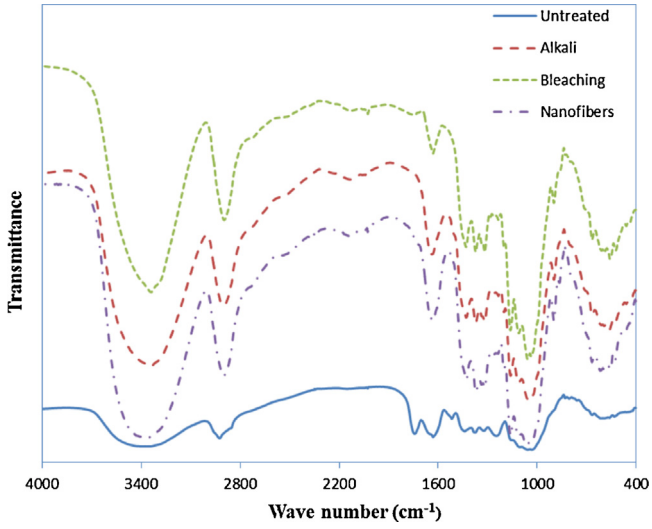

Fig. 4. FTIR spectra of the untreated DSBP, alkali treated DSBP, bleached DSBP, and cellulose nanofibers.

of untreated SBP and treated SBP and it indicates the hydrophilic nature in both the untreated and untreated SBP (Kaushik & Singh, 2011). The prominent peak at 2924 cm^{-1} is due to the stretching vibration of saturated C—H in cellulose, hemicellulose, and lignin (Alemdar & Sain, 2008; Kaushik & Singh, 2011). The prominent peak at 1630 cm^{-1} is principally associated with the bending vibration of absorbed water molecules. The blending vibration of C—H gets reflected in two peaks at 1371 cm^{-1} and 1443 cm^{-1} due to asymmetric and symmetric bending vibrations, respectively (Sain & Panthapulakkal, 2006; Xiao, Sun, & Sun, 2001).

A shoulder located at 1745 cm^{-1} in the spectrum of untreated SBP can be attributed to the stretching vibration of carbonyl groups representing the acetyl and uronic ester groups in hemicellulose. This shoulder can also be attributed to the ester linkage of carboxylic group of p-coumaric and ferulic acids which are dominant constituents of hemicellulose and/or lignin (Alemdar & Sain, 2008). This peak (1745 cm^{-1}) has disappeared in the FTIR spectrum of SBP after alkali and bleaching treatments. These results indicate that the hemicellulose and lignin contents were removed from the untreated SBP during chemical treatments. However, the data presented in Table 1 show that the hemicellulose and lignin contents were not entirely removed by these chemical treatments. This observation suggests that the absence of carbonyl groups in the FTIR spectrum most probably is due to the cleavage of ester bond and carboxylic group in hemicellulose and/or lignin.

The C=C stretching vibration of aromatic ring in lignin causes skeletal vibration of the ring. A distinct characteristic peak that appears at 1517 cm^{-1} in untreated SBP can be assigned to the C=C stretching of lignin (Xiao et al., 2001). The peak height at 1517 cm^{-1} has decreased but it still appeared in the alkali treated SBP and finally disappeared in the bleached SBP. These results suggest that the alkali treatment did not effectively remove the lignin and that the subsequent bleaching treatment caused further removal of lignin. The broad peak observed at 1240 cm^{-1} representing the absorption of ester has significantly decreased after the chemical treatments. The peak at 1035 cm^{-1} due to ether linkage (C—O—C) in hemicellulose has also weakened after the chemical treatments (Cherian et al., 2008). These observations indicate that most of the hemicellulose content was removed and a small amount of hemicellulose was still remained during the chemical treatments. These observations are corroborated by the chemical composition data presented in Table 1. The bands at 1058 cm^{-1} and 898 cm^{-1} appearing in all spectra are assigned to C-O stretching and the glycosidic C—H rock vibration both of which are characteristic of the cellulose structure (Sun, Tomkinson, Wang, & Xiao, 2000). However, the intensity of these two peaks has increased in treated SBP indicating that the treated SBP contained better enriched cellulose. These results indicate that the hemicellulose and lignin were successfully removed to a great extent during the chemical treatments.

No significant difference was found between the spectra of bleached DSBP and cellulose nanofibers. These results indicated that chemical structure did not change in the samples after HPH treatment.

3.4. X-ray diffraction analysis

As shown in Table 1, the untreated SBP consists of three major components: cellulose, hemicellulose, and lignin. It is commonly accepted that the cellulose fibers are crystalline in nature. This crystalline structure of cellulose fibers is interrupted by hemicellulose and they are also embedded in the lignin matrix. The intermolecular hydrogen bonds between the cellulose molecules give rise to the crystalline structure of cellulose in lignocellulosic biomass (Alemdar & Sain, 2008). Hence, it is expected that the crystallinity of cellulose fibers increases when the hemicellulose and lignin are progressively removed. The chemical treatments which are capable

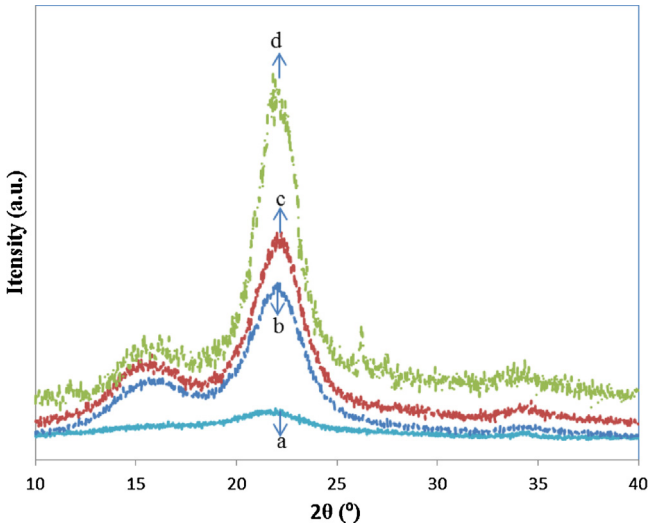

Fig. 5. X-ray diffraction patterns of (a) the untreated DSBP, (b) alkali treated DSBP, (c) bleached DSBP, and (d) cellulose nanofibers.

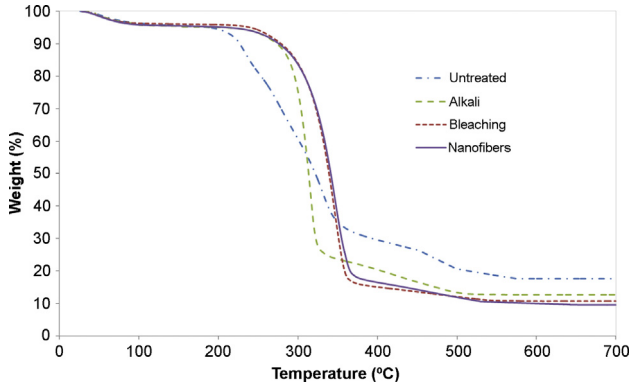

Fig. 6. Mass loss (%) kinetics of untreated DSBP, alkali treated DSBP, bleached DSBP, and cellulose nanofibers obtained using TGA.

of removing the non-cellulosic biomass can affect the crystallinity of the cellulose.

The X-ray diffraction patterns of untreated SBP fibers, chemically treated fibers and cellulose nanofibers are shown in Fig. 5. As can be seen from this figure, all the samples exhibit a sharp diffraction peak at 22° (2θ) which is characteristic of typical cellulose I structure (Nishiyama, Sugiyama, Chanzy, & Langan, 2003). This diffraction peak indicates that the crystal structure in the chemically treated samples has remained intact. The diffraction peak at 22° (2θ) is quite broad in the case of untreated DSBP. This peak in the case of chemically treated SBP is much sharper and narrower compared to that of untreated SBP. This result indicates that the chemically treated samples have higher degree of crystallinity. It can also be seen from the diffractogram of cellulose, the sharpness in the edge of the diffractogram of nanofibers has greatly increased. A more obvious shoulder peak at 16° (2θ) observed after the chemical treatments can be attributed to the highly enriched structure of cellulose. The enrichment in cellulose is due to the efficient removal of amorphous fraction from the de-pectinated sugar beet pulp.

The crystallinity index (CI) is related to the strength and stiffness of fibers (Wang, Han, & Zhang, 2007). The CI was calculated according to Segal et al. (1959)'s method (Section 2.3.4) which provides a quantitative measure of the crystallinity in powders. It can be seen from Table 1 that the CI values were 35.67%, 66.87%, 69.62%, and 77.89% for the untreated DSBP, alkali treated DSBP, bleached DSBP, and cellulose nanofibers, respectively. These data indicate that the crystallinity was significantly ($p < 0.05$) increased when the untreated DSBP was converted into cellulose nanofibers. This extent of increase of crystallinity in chemically treated DSBP compared to the untreated DSBP can be attributed to the efficient removal of hemicellulose and lignin from the amorphous regions and enrichment of cellulose content in DSBP due to alkali and bleaching treatments. The application of high pressure homogenization (HPH) further increased the crystallinity of cellulose nanofibers to 77.89%. This indicates that the HPH breaks the amorphous regions and reorganizes and enriches the semicrystalline cellulose regions. This result is in accordance with that of Lu, Gui, Zheng, and Liu (2013) who reported that the crystallinity of cellulose fibers increased from 59.79% to 70.26% after micronization. The increase in the percentage of crystallinity increases the tensile strength and rigidity of cellulose fibers due to the greatly ordered and compact molecular structure among cellulose molecules. The greater enrichment of cellulose increases the Young's modulus in the crystalline region along the longitudinal direction (Sakurada, Nukushina, & Ito, 1962). Therefore, cellulose nanofibers obtained from combined application of chemical treatments and high pressure homogenization treatment could be highly effective in achieving better reinforcement in composite materials.

3.5. Thermal stability analysis

The thermal stability of DSBP fibers is very important for their greater application in reinforced-biocomposite materials because typical processing temperature for many thermoplastics exceeds 200 °C (Tadmor & Gogos, 1979). Fig. 6 and Table 2 show the TGA results obtained from untreated, alkali treated, bleached and HPH treated DSBP fibers. As can be seen from this figure, there is only a small mass loss when these samples are heated from 30 to 150 °C. This mass loss in the early stage corresponds to the evaporation of water content and to some extent loss of low molecular weight compounds which exist in untreated DSBP (Morán, Alvarez, Cyras, & Vázquez, 2008). The degradation kinetics of untreated, chemically treated and HPH treated samples have two main characteristic features which has reflected into the decomposition occurring in the two stages (Fig. 6). Fig. 6 also shows that the degradation temperatures of DSBP fibers greatly increased after chemical and HPH treatments. For example, the untreated DSBP fibers started to degrade at 224.4 °C, while the alkali treated samples began to decompose at 258.3 °C (Fig. 6 and Table 2). The higher degradation temperature in alkali treated DSBP fibers indicates that the alkali treated DSBP fibers have much higher thermal stability compared to that of the untreated DSBP fibers. This is because substantial proportion of pectin, hemicellulose and lignin is present in the untreated DSBP which are known to have lower thermal stability than cellulose (Chen et al., 2011). The data presented in Fig. 6 and Table 2 also shows that the thermal degradation temperature of bleached fibers is 271.7 °C which is higher than that of alkali treated fibers. This indicates that the further removal of non-cellulosic impurities by bleaching process is conducive in improving the thermal stability of DSBP cellulose fibers. Overall, the thermal degradation data presented in Fig. 6 show conclusively that the chemically treated DSBP fibers have a better thermal stability compared to untreated ones. This is because substantial amount of non-cellulosic materials were dissolved and were subsequently removed during the sequential chemical treatments. Yet another reason is that the chemically treated samples were repeatedly washed and filtered which further removed the calcium oxalate and other water soluble salts (Alemdar & Sain, 2008). The high thermal degradation temperature of cellulose nanofibers can broaden their applicability as biocompatible materials especially in high temperature applications (>200 °C) (Kaushik & Singh, 2011).

Table 2
Crystallinity index (CI) and degradation characteristics of DSBP at different stages of treatment.

Materials	Relative crystallinity (%)	Onset of degradation (°C)	Residue when treated at 600 °C (%)
Untreated fibers	39.96	224.4	17.67
Alkali treated fibers	66.87	258.3	12.78
Bleached fibers	69.62	271.1	11.7
Cellulose nanofibers	77.89	272.7	10.73

When the chemically treated and untreated DSBP fibers were heated to 600 °C, the amount of the residue left behind was quite different (Table 2). The amount of residue in the case of untreated DSBP fibers when heated at 600 °C was 17.7%. The alkali treated DSBP had significantly ($p < 0.05$) lower residues (12.78%) compared to that of the untreated DSBP which can be attributed to the efficient removal of hemicellulose, lignin and SiO_2. The amount of residues of bleached DSBP cellulose fibers further decreased to 11.7%. This is because bleaching treatment removed the lignin and hemicellulose contents further.

4. Conclusions

Cellulose nanofibers were successfully prepared from depectinated sugar beet pulp (DSBP) using chemical (alkali and bleaching) treatments and high pressure homogenization. Chemical composition, morphological features, crystallinity and thermal degradation characteristics of the resultant cellulose fibers and cellulose nanofibers were characterized by using FTIR, SEM, TEM, XRD, and TGA. Chemical and FTIR analysis revealed that chemical treatments were quite efficient in removing hemicellulose and lignin contents of the DSBP due to which the cellulose contents increased from 44.96% to 82.83%. The application of HPH disrupted the cell wall and helped in the release of the cellulose nanofibers. The diameter of cellulose nanofibers after HPH treatment ranged from <10 nm to 70 nm. The crystallinity index of cellulose nanofibers increased from 35.67% to 77.89% due to the dissolution of amorphous fraction. The cellulose nanofibers had significantly ($p < 0.05$) better thermal stability (thermal degradation temperature = 271.7 °C) compared to that of the untreated DSBP (thermal degradation temperature = 224.4 °C). These DSBP cellulose nanofibers can be preferably used as a biocompatible material at high temperature applications.

Acknowledgments

This research was supported by Beijing Municipal Science and Technology Commission Project (Z121100001312010 and D12110003112002), National Natural Science Foundation of China (31000813), High Technology Research and Development Program of China (2011AA100802), Science and Technology Support Project of China (2013BAD10B03), Commonweal Guild Agricultural Scientific Research Program of China (201003077), and Chinese Universities Scientific Fund (2012YJ092, 2012QJ009, and 2013YJ007).

References

Abe, K., Iwamoto, S., & Yano, H. (2007). Obtaining cellulose nanofibers with a uniform width of 15 nm from wood. *Biomacromolecules*, *8*(10), 3276–3278.
Abe, K., & Yano, H. (2009). Comparison of the characteristics of cellulose microfibril aggregates of wood, rice straw and potato tuber. *Cellulose*, *16*(6), 1017–1023.
Alemdar, A., & Sain, M. (2008). Isolation and characterization of nanofibers from agricultural residues – Wheat straw and soy hulls. *Bioresource Technology*, *99*(6), 1664–1671.
Azizi Samir, M. A. S., Alloin, F., & Dufresne, A. (2005). Review of recent research into cellulosic whiskers, their properties and their application in nanocomposite field. *Biomacromolecules*, *6*(2), 612–626.
Bradley, E. L., Castle, L., & Chaudhry, Q. (2011). Applications of nanomaterials in food packaging with a consideration of opportunities for developing countries. *Trends in Food Science and Technology*, *22*(11), 604–610.
Chen, W., Yu, H., Liu, Y., Hai, Y., Zhang, M., & Chen, P. (2011). Isolation and characterization of cellulose nanofibers from four plant cellulose fibers using a chemical-ultrasonic process. *Cellulose*, *18*(2), 433–442.
Cherian, B. M., Pothan, L. A., Nguyen-Chung, T., Mennig, G., Kottaisamy, M., & Thomas, S. (2008). A novel method for the synthesis of cellulose nanofibril whiskers from banana fibers and characterization. *Journal of Agricultural and Food Chemistry*, *56*(14), 5617–5627.
Corrêa, A. C., de Morais Teixeira, E., Pessan, L. A., & Mattoso, L. H. C. (2010). Cellulose nanofibers from curaua fibers. *Cellulose*, *17*(6), 1183–1192.
Faruk, O., Bledzki, A. K., Fink, H., & Sain, M. (2012). Biocomposites reinforced with natural fibers: 2000–2010. *Progress in Polymer Science*, *37*(11), 1552–1596.
Iwamoto, S., Abe, K., & Yano, H. (2008). The effect of hemicelluloses on wood pulp nanofibrillation and nanofiber network characteristics. *Biomacromolecules*, *9*(3), 1022–1026.
Jin, Y. Z. (2004). Depth development on beet pulp. *China Beet and Sugar*, (3), 16–18.
Johar, N., Ahmad, I., & Dufresne, A. (2012). Extraction, preparation and characterization of cellulose fibres and nanocrystals from rice husk. *Industrial Crops and Products*, *37*(1), 93–99.
Jonoobi, M., Harun, J., Mathew, A. P., Hussein, M. Z. B., & Oksman, K. (2010). Preparation of cellulose nanofibers with hydrophobic surface characteristics. *Cellulose*, *17*(2), 299–307.
Kaliyan, N., & Vance Morey, R. (2009). Factors affecting strength and durability of densified biomass products. *Biomass and Bioenergy*, *33*(3), 337–359.
Kaushik, A., & Singh, M. (2011). Isolation and characterization of cellulose nanofibrils from wheat straw using steam explosion coupled with high shear homogenization. *Carbohydrate Research*, *346*(1), 76–85.
Kim, J., Yun, S., & Ounaies, Z. (2006). Discovery of cellulose as a smart material. *Macromolecules*, *39*(12), 4202–4206.
Lu, H., Gui, Y., Zheng, L., & Liu, X. (2013). Morphological, crystalline, thermal and physicochemical properties of cellulose nanocrystals obtained from sweet potato residue. *Food Research International*, *50*(1), 121–128.
Lv, C., Wang, Y., Wang, L., Li, D., & Adhikari, B. (2013). Optimization of production yield and functional properties of pectin extracted from sugar beet pulp. *Carbohydrate Polymers*, *95*(1), 233–240.
Morán, J. I., Alvarez, V. A., Cyras, V. P., & Vázquez, A. (2008). Extraction of cellulose and preparation of nanocellulose from sisal fibers. *Cellulose*, *15*(1), 149–159.
Nakagaito, A. N., & Yano, H. (2008). Toughness enhancement of cellulose nanocomposites by alkali treatment of the reinforcing cellulose nanofibers. *Cellulose*, *15*(2), 323–331.
Nishino, T., Matsuda, I., & Hirao, K. (2004). All-cellulose composite. *Macromolecules*, *37*(20), 7683–7687.
Nishiyama, Y., Sugiyama, J., Chanzy, H., & Langan, P. (2003). Crystal structure and hydrogen bonding system in cellulose I_α from synchrotron X-ray and neutron fiber diffraction. *Journal of the American Chemical Society*, *125*(47), 14300–14306.
Nogi, M., Iwamoto, S., Nakagaito, A. N., & Yano, H. (2009). Optically transparent nanofiber paper. *Advanced Materials*, *21*(16), 1595–1598.
Okiyama, A., Motoki, M., & Yamanaka, S. (1993). Bacterial cellulose IV. Application to processed foods. *Food Hydrocolloids*, *6*(6), 503–511.
Pääkkö, M., Ankerfors, M., Kosonen, H., Nykänen, A., Ahola, S., Österberg, M., et al. (2007). Enzymatic hydrolysis combined with mechanical shearing and high-pressure homogenization for nanoscale cellulose fibrils and strong gels. *Biomacromolecules*, *8*(6), 1934–1941.
Rosa, M. F., Medeiros, E. S., Malmonge, J. A., Gregorski, K. S., Wood, D. F., Mattoso, L. H. C., et al. (2010). Cellulose nanowhiskers from coconut husk fibers: effect of preparation conditions on their thermal and morphological behavior. *Carbohydrate Polymers*, *81*(1), 83–92.
Sain, M., & Panthapulakkal, S. (2006). Bioprocess preparation of wheat straw fibers and their characterization. *Industrial Crops and Products*, *23*(1), 1–8.
Sakurada, I., Nukushina, Y., & Ito, T. (1962). Experimental determination of the elastic modulus of crystalline regions in oriented polymers. *Journal of Polymer Science: Part A: Polymer Chemistry*, *57*(165), 651–660.
Segal, L., Creely, J. J., Martin, A. E., & Conrad, C. M. (1959). An empirical method for estimating the degree of crystallinity of native cellulose using the X-ray diffractometer. *Textile Research Journal*, *29*(10), 786–794.
Siqueira, G., Bras, J., & Dufresne, A. (2008). Cellulose whiskers versus microfibrils: Influence of the nature of the nanoparticle and its surface functionalization on the thermal and mechanical properties of nanocomposites. *Biomacromolecules*, *10*(2), 425–432.

Soykeabkaew, N., Supaphol, P., & Rujiravanit, R. (2004). Preparation and characterization of jute- and flax-reinforced starch-based composite foams. *Carbohydrate Polymers*, *58*(1), 53–63.

Sun, R. C., Tomkinson, J., Wang, Y. X., & Xiao, B. (2000). Physico-chemical and structural characterization of hemicelluloses from wheat straw by alkaline peroxide extraction. *Polymer*, *41*(7), 2647–2656.

Syverud, K., Chinga-Carrasco, G., Toledo, J., & Toledo, P. G. (2011). A comparative study of *Eucalyptus* and *Pinus radiata* pulp fibres as raw materials for production of cellulose nanofibrils. *Carbohydrate Polymers*, *84*(3), 1033–1038.

Tadmor, Z., & Gogos, C. G. (1979). *Principles of polymer processing*. New York: John Wiley and Sons.

Thiripura Sundari, M., & Ramesh, A. (2012). Isolation and characterization of cellulose nanofibers from the aquatic weed water hyacinth – *Eichhornia crassipes*. *Carbohydrate Polymers*, *87*(2), 1701–1705.

Villanova, J. C. O., Ayres, E., Carvalho, S. M., Patrício, P. S., Pereira, F. V., & Oréfice, R. L. (2011). Pharmaceutical acrylic beads obtained by suspension polymerization containing cellulose nanowhiskers as excipient for drug delivery. *European Journal of Pharmaceutical Sciences*, *42*(4), 406–415.

Wang, B., Li, D., Wang, L., Liu, Y., & Adhikari, B. (2012). Effect of high-pressure homogenization on microstructure and rheological properties of alkali-treated high-amylose maize starch. *Journal of Food Engineering*, *113*(1), 61–68.

Wang, L., Han, G., & Zhang, Y. (2007). Comparative study of composition, structure and properties of *Apocynum venetum* fibers under different pretreatments. *Carbohydrate Polymers*, *69*(2), 391–397.

Wise, L. E., Murphy, M., & D'Addieco, A. A. (1946). Chlorite holocellulose, its fractionation and bearing on summative wood analysis and on studies on the hemicelluloses. *Technical Association Papers*, *29*(6), 210–218.

Xiao, B., Sun, X. F., & Sun, R. (2001). Chemical, structural, and thermal characterizations of alkali-soluble lignins and hemicelluloses, and cellulose from maize stems, rye straw, and rice straw. *Polymer Degradation and Stability*, *74*(2), 307–319.